2014

Targeting an IKBKE cytokine network impairs triple-negative breast cancer growth

Thanh U. Barbie
Washington University School of Medicine in St. Louis

Shunqiang Li
Washington University School of Medicine in St. Louis

Xiuli Zhang
Washington University School of Medicine in St. Louis

John Herndon
Washington University School of Medicine in St. Louis

Timothy Fleming
Washington University School of Medicine in St. Louis

See next page for additional authors

Targeting an IKBKE cytokine network impairs triple-negative breast cancer growth

Thanh U. Barbie,[1,2] Gabriela Alexe,[3,4,5] Amir R. Aref,[6] Shunqiang Li,[2,7] Zehua Zhu,[3,6] Xiuli Zhang,[1] Yu Imamura,[6] Tran C. Thai,[3,6] Ying Huang,[6] Michaela Bowden,[6] John Herndon,[1] Travis J. Cohoon,[6] Timothy Fleming,[1,2] Pablo Tamayo,[3] Jill P. Mesirov,[3] Shuji Ogino,[6] Kwok-Kin Wong,[6] Matthew J. Ellis,[2,7] William C. Hahn,[3,6] David A. Barbie,[3,6] and William E. Gillanders[1,2]

[1]Department of Surgery, Division of Biology and Biomedical Sciences, and [2]Alvin J. Siteman Cancer Center, Washington University, St. Louis, Missouri, USA. [3]Broad Institute of Harvard and MIT, Cambridge, Massachusetts, USA. [4]Department of Pediatric Oncology, Dana-Farber Cancer Institute and Boston Children's Hospital, Harvard Medical School, Boston, Massachusetts, USA. [5]Graduate Program in Bioinformatics, Boston University, Boston, Massachusetts, USA. [6]Department of Medical Oncology and Cancer Biology, Dana-Farber Cancer Institute, Boston, Massachusetts, USA. [7]Division of Medical Oncology, Washington University, St. Louis, Missouri, USA.

Triple-negative breast cancers (TNBCs) are a heterogeneous set of cancers that are defined by the absence of hormone receptor expression and *HER2* amplification. Here, we found that inducible IκB kinase–related (IKK-related) kinase IKBKE expression and JAK/STAT pathway activation compose a cytokine signaling network in the immune-activated subset of TNBC. We found that treatment of cultured IKBKE-driven breast cancer cells with CYT387, a potent inhibitor of TBK1/IKBKE and JAK signaling, impairs proliferation, while inhibition of JAK alone does not. CYT387 treatment inhibited activation of both NF-κB and STAT and disrupted expression of the protumorigenic cytokines CCL5 and IL-6 in these IKBKE-driven breast cancer cells. Moreover, in 3D culture models, the addition of CCL5 and IL-6 to the media not only promoted tumor spheroid dispersal but also stimulated proliferation and migration of endothelial cells. Interruption of cytokine signaling by CYT387 in vivo impaired the growth of an IKBKE-driven TNBC cell line and patient-derived xenografts (PDXs). A combination of CYT387 therapy with a MEK inhibitor was particularly effective, abrogating tumor growth and angiogenesis in an aggressive PDX model of TNBC. Together, these findings reveal that IKBKE-associated cytokine signaling promotes tumorigenicity of immune-driven TNBC and identify a potential therapeutic strategy using clinically available compounds.

Introduction

Advances in targeted therapy for patients with breast cancers that express estrogen/progesterone receptors and/or *HER2* have improved patient outcomes and survival. Limited treatment options exist, however, for the 15% to 20% of patients with triple-negative breast cancers (TNBCs). Although TNBCs may respond to anthracycline-based chemotherapy or cisplatin, tumors frequently relapse, resulting in decreased disease-free and overall survival compared with other breast cancer subtypes (1).

The diversity of somatic mutations, gene amplifications, and deletions observed in TNBC has hampered efforts to elucidate a common drug target in this breast cancer subtype (2). Recent evidence suggests that a significant fraction of TNBCs exhibit immune cell infiltration, with features of stem cells and epithelial-mesenchymal transition (3–5). Indeed, a refined classification of TNBC based on gene expression profiling recently identified an immunomodulatory (IM) subtype that corresponds with this category of tumors (6). However, the specific genetic drivers of this and other TNBC subtypes remain poorly defined.

The IκB kinase–related (IKK-related) kinases TANK-binding kinase 1 (TBK1) and IκB kinase ε (IKBKE, also known as IKKε) represent an emerging link between inflammation and cancer (7). In response to pathogen exposure, induction of IKBKE reinforces TBK1 signaling and promotes sustained activation of the type 1 interferon pathway (8–11). Furthermore, IKBKE directly phosphorylates and activates specific STAT transcription factors (12, 13), and cytokines produced by TBK1/IKBKE can engage downstream JAK/STAT signaling in an autocrine or paracrine fashion (14).

IKBKE is also aberrantly expressed and/or amplified in approximately 30% of breast carcinomas (15–17), in which it induces survival signaling associated with NF-κB pathway activation. IKBKE activation facilitates cell transformation, whereas suppression of *IKBKE* in breast cancer cell lines that harbor *IKBKE* amplification or overexpression results in cell death (16). IKBKE phosphorylates CYLD and TRAF2 in breast cancer cells, which induces NF-κB activation and contributes to cell transformation (18, 19). However, a comprehensive understanding of how IKBKE promotes tumorigenicity is lacking, and the therapeutic efficacy of targeting IKBKE signaling in vivo has yet to be defined.

Activation of NF-κB and JAK/STAT signaling has been strongly implicated in the pathogenesis of certain TNBCs and closely related basal-like breast cancers (20–24). Markers of JAK/STAT pathway activation are particularly enriched in the IM TNBC gene expres-

Conflict of interest: David A. Barbie is a consultant for N-of-One. William C. Hahn is a consultant for Novartis.
Submitted: February 19, 2014; **Accepted:** September 30, 2014.
Reference information: *J Clin Invest*. 2014;124(12):5411–5423. doi:10.1172/JCI75661.

Table 1. *IKBKE* copy number in ZR-751– and IKBKE-expressing TNBC cell lines from the Broad/Novartis Cell Line Encyclopedia

Cell line	*IKBKE* CN (log_2 [CN/2])
ZR751	1.23
MDA-MB-231	0.12
MDA-MB-468	0.36
HCC70	0.47
HCC1143	0.49
HCC1187	0.53

CN, copy number.

sion subtype (6). Here, we report that, in addition to its genomic amplification in luminal breast tumors, IKBKE is aberrantly overexpressed in TNBC and coordinately activates NF-κB, STAT, and cytokine signaling in this subset of cancers. Furthermore, we identify combined TBK1/IKBKE, JAK, and MEK inhibition as a novel potent therapeutic strategy for this class of tumors.

Results

Identification of an IKBKE-driven TNBC subtype. *IKBKE* is amplified in approximately 30% of human breast tumors, and luminal breast cancer cell lines that harbor *IKBKE* copy gain are dependent upon its expression (16). *IKBKE* overexpression has also been observed in breast cell lines and cancers without *IKBKE* amplification, such as the TNBC cell lines, MDA-MB-231 and MDA-MB-468 (17). To gain further insight into IKBKE regulation and function in breast cancer, we analyzed gene expression data from primary breast cancers profiled in the The Cancer Genome Atlas (TCGA) data set (2). Whereas *IKBKE* expression was linked with *IKBKE* amplification in luminal tumors, a substantial additional fraction of breast cancers overexpressed *IKBKE* in the absence of gene amplification (Figure 1A). Since IKBKE is also induced by multiple different cytokines (25), we examined correlation between the levels of several different cytokine gene expression signatures and *IKBKE* mRNA expression across these samples (26, 27). Among these signatures, IL-1 induction correlated most strongly with high *IKBKE* levels in a subtype of TNBC, followed by *TNFA* ($P < 0.001$ for both, normalized mutual information (NMI) statistic) (Figure 1A and Supplemental Figure 1, A and B). Hierarchical clustering with previously reported gene expression subtypes (6) and B lymphocyte markers (28) further revealed that *IKBKE* expression and IL-1 activation most closely associated with the IM subtype of TNBC and with lymphocytic infiltration ($P < 0.001$ and $P < 0.02$, respectively, NMI statistic) (Supplemental Figure 1C). *IKBKE* mRNA levels correlated with mutant *TP53* status across all TCGA tumors, but this did not reach statistical significance within the TNBC subset (Supplemental Figure 2A). Response to neoadjuvant cisplatin therapy failed to correlate with *IKBKE* expression status in another cohort of patients with TNBC (Supplemental Figure 2A).

To explore this observation further, we next identified cell lines that express elevated *IKBKE* levels using gene expression data from the Broad/Novartis Cell Line Encyclopedia (29). Similar to ZR751, a luminal breast cancer cell line that harbors *IKBKE* copy number gain (16), and in contrast to $HER2^+$ BT474 cells or nontransformed MCF-10A cells, we identified several TNBC cell lines that expressed high levels of IKBKE protein (Figure 1B). Whereas ZR751 cells exhibited copy number gain at the *IKBKE* locus as expected, multiple IKBKE-expressing TNBC cell lines failed to show evidence of genomic *IKBKE* amplification (Table 1). These findings recapitulated what we had observed in primary tumors and confirmed that *IKBKE* is not only amplified in luminal breast cancers but also aberrantly overexpressed in a subset of TNBC.

IKBKE-amplified ZR751 cells depend on IKBKE expression for their proliferation and survival (16). Using 2 independent *IKBKE*-specific shRNAs, we found that TNBC MDA-MB-468 cells were at least as sensitive to suppression of *IKBKE* as ZR751 cells (Figure 1C). Indeed, whereas specific depletion of IKBKE failed to affect the proliferation of nontransformed MCF10A cells, we confirmed that suppression of *IKBKE* expression inhibited the proliferation of multiple IKBKE-amplified (ZR751 and MCF7) and *IKBKE*-overexpressing TNBC cell lines (MDA-MB-231 and MDA-MB-468) (Figure 1D). These findings revealed that *IKBKE* is not only overexpressed but also contributes to the proliferation and survival of this subset of TNBC.

IKBKE expression in TNBC is associated with STAT3 activation and cytokine production. IKBKE promotes NF-κB (7) and STAT signaling (12, 13) both directly and indirectly via autocrine cytokine production (14). Indeed, we confirmed that *IKBKE* overexpression in HEK-293T (293T) cells not only induced NF-κB pathway activation, as measured by S933 phosphorylated NF-κB p105 levels, but also STAT3 activation, as reflected by increased Y705 phosphorylated STAT3 (pSTAT3) levels (Figure 2A). Activation of these signaling pathways by IKBKE was associated with induction of *CCL5* expression in a kinase-dependent manner (Figure 2B). When we measured IKBKE levels and activated STAT3 (as measured by Y705 pSTAT3 levels) across breast cancer cell lines, we observed correlation preferentially in TNBC cell lines (Figure 2C). These findings suggested that engagement of IKBKE signaling in TNBC occurred within the context of a broader cytokine signaling network. Since elevated *IKBKE* expression in TNBC tumors correlated with IL-1 and other markers of inflammation (Figure 1A and Supplemental Figures 1, A–C), we assessed the role of IL-1β in engaging IKBKE signaling in this context. Indeed, treatment of multiple TNBC cell lines with IL-1β led to a substantial further increase in IKBKE protein levels (Figure 2D) and enhanced the secretion of CCL5 (Figure 2E). Depletion of IKBKE alone in MDA-MB-468 cells failed to prevent IL-1β–induced CCL5 production but modestly reduced IL-6 levels (Supplemental Figure 3, A and B). These observations support the view that functional redundancy exists between multiple components of this network, including TBK1, which together with IKBKE promotes CCL5 and IL-6 production (30).

Sensitivity of IKBKE-driven TNBC cells to CYT387 treatment. We next compared the effects of selective inhibition of JAK/STAT signaling on TNBC cell proliferation and survival by treatment with the JAK inhibitor ruxolitinib (31) or the multitargeted JAK/TBK1/IKBKE inhibitor CYT387 (30, 32, 33). Treatment of MDA-MB-468 cells with ruxolitinib or CYT387 over a range of doses inhibited STAT3 phosphorylation (Figure 3A). Despite comparable inhibition of JAK signaling, treatment of these cells with CYT387 but not ruxolitinib impaired the viability of multiple different TNBC cell lines (Figure 3, B and C).

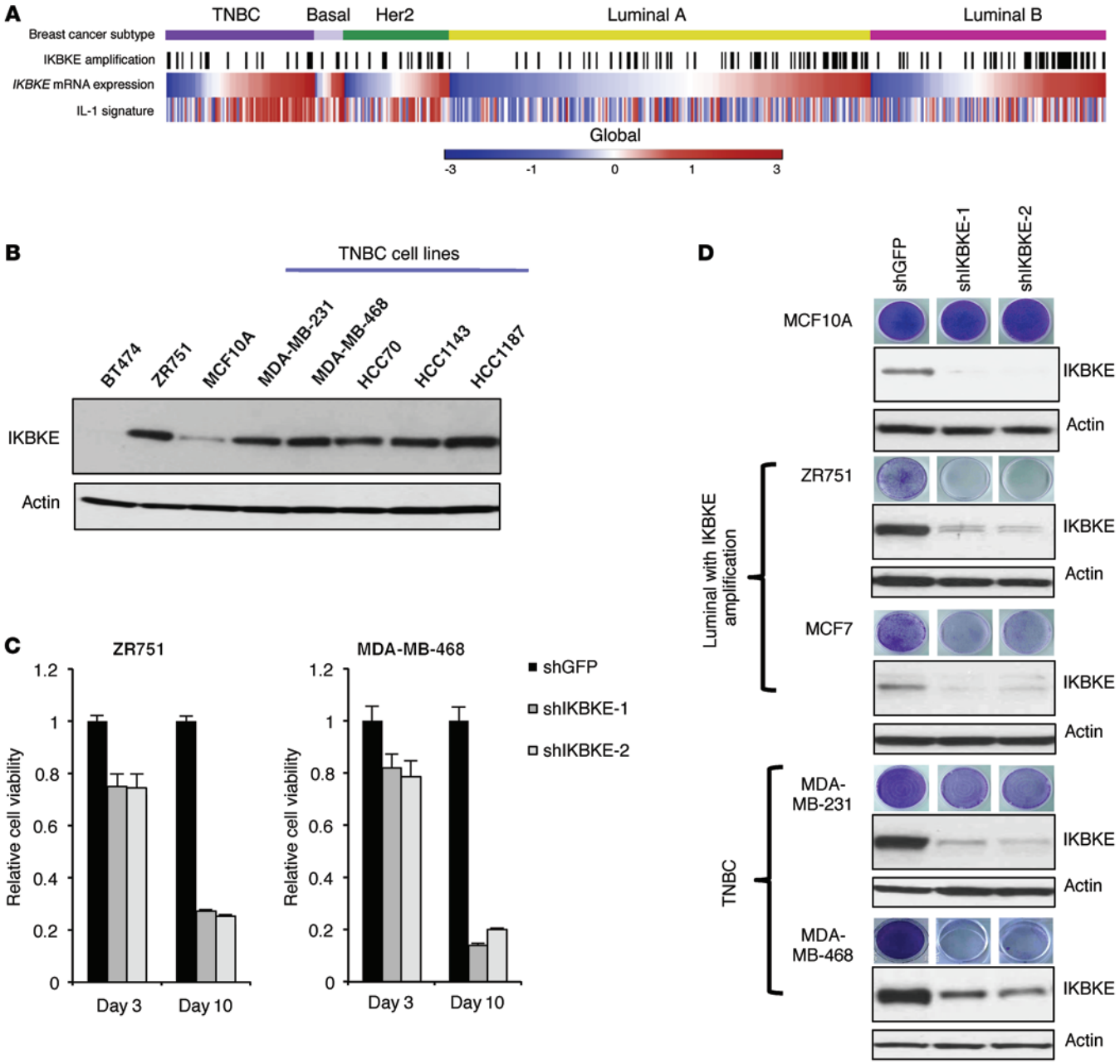

Figure 1. IKBKE overexpression defines a subset of TNBCs. (**A**) *IKBKE* amplification and mRNA expression in the TCGA breast cancer data set, compared with IL-1 signature enrichment by single-sample gene set enrichment analysis (ssGSEA). Light purple represents basal but progesterone receptor–positive tumors. Black lines indicate IKBKE amplification on 1q32, red indicates high expression, and blue indicates low expression. (**B**) Immunoblot of IKBKE and β-actin levels across a panel of TNBC cell lines compared with BT474 (HER2$^+$), ZR-751 (luminal, IKBKE-amplified), and MCF-10A (basal-like, nontransformed) cells. (**C**) Relative cell viability by CellTiter-Glo (CTG) Luminescent Cell Viability Assay on day 3 or day 10 following expression of 2 different IKBKE shRNAs compared with shGFP control in ZR-751 or MDA-MB-468 cells. Values represent mean and SEM of triplicate samples. (**D**) Crystal violet–stained cells and immunoblots of IKBKE and β-actin levels from parallel wells following control shGFP expression or that of 2 different IKBKE-specific shRNAs in the indicated cell lines.

We further examined the effects of CYT387 treatment on MDA-MB-468 cells in a 3D culture tumor spheroid dispersal assay that captures features of the tumor microenvironment and also models aspects of the epithelial-mesenchymal transition (34). EGF-induced proliferation of MDA-MB-468 breast cancer cells in this assay was completely suppressed by CYT387 treatment at concentrations as low as 800 nM (Supplemental Figure 4A). We also cultured several other TNBC cell lines in 3D suspension together with IL-1β and found that CYT387 treatment inhibited proliferation and caused cells to aggregate (Supplemental Figure 4B). These findings demonstrate that CYT387 treatment uniquely impairs not only cell viability in 2D culture but also growth factor– and cytokine-driven TNBC cell proliferation and dispersal in 3D culture.

Next, we treated a panel of 15 breast cancer cell lines with CYT387 over a range of concentrations and found that TNBCs that exhibited high levels of IKBKE and pSTAT3 exhibited the greatest sensitivity,

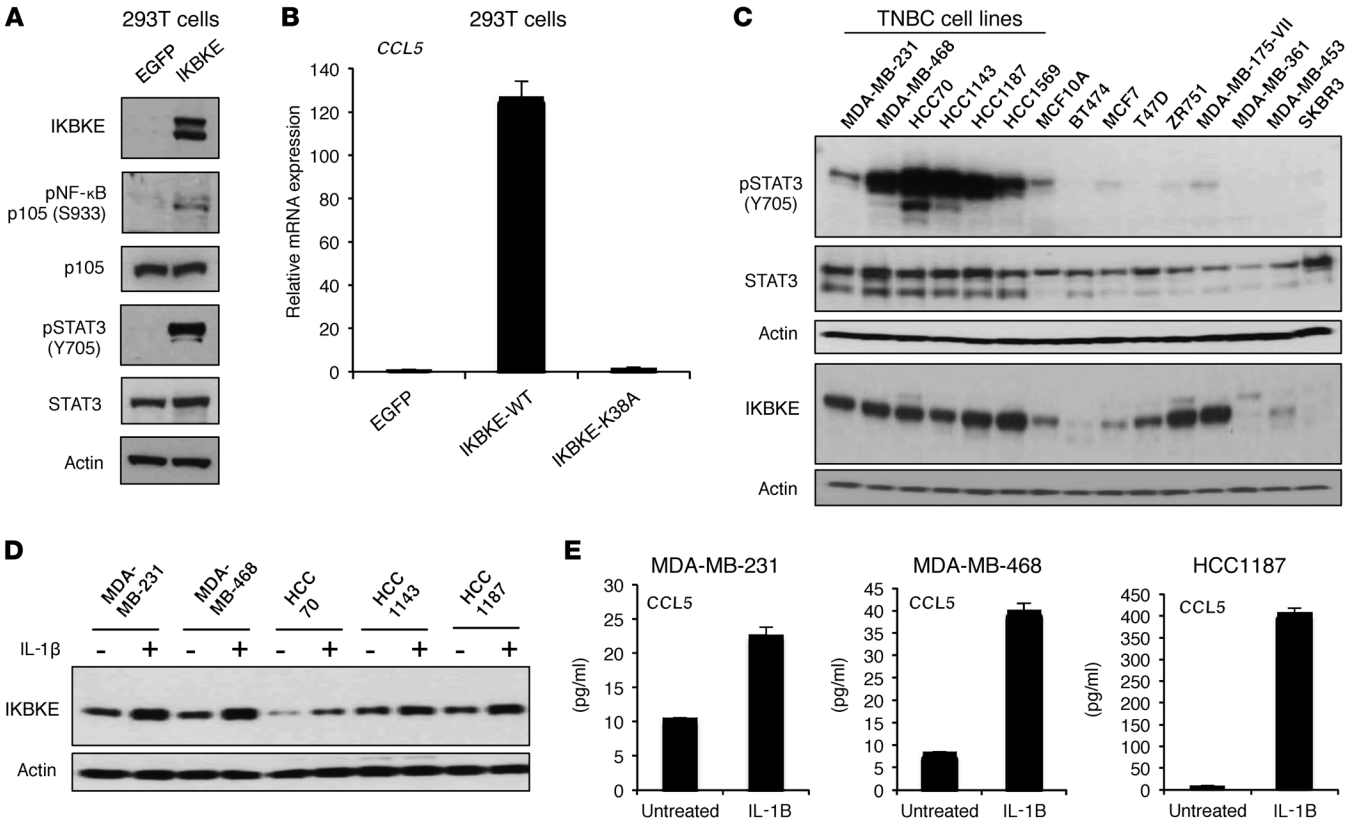

Figure 2. IKBKE promotes inflammatory signaling and is induced by IL-1 in TNBC cells. (**A**) Immunoblot of IKBKE, S933 p-p105, total p105, Y705 pSTAT3, total STAT3, and β-actin in 293T cells transiently transfected with IKBKE or a control EGFP-expressing vector. (**B**) *CCL5* mRNA expression in 293T cells following transient transfection with EGFP, IKBKE-WT, and IKBKE-K38A. Values were normalized to EGFP and represent the mean and SEM of triplicate samples. (**C**) Immunoblot of IKBKE, Y705 pSTAT3, total STAT3, and β-actin in a panel of 15 breast cancer cell lines. (**D**) Immunoblot of IKBKE and β-actin in a panel of TNBC cell lines with or without exogenous IL-1β (25 ng/ml) for 24 hours. (**E**) CCL5 levels in the media measured by ELISA following IL-1β (25 ng/ml) treatment of IKBKE-expressing TNBC cell lines for 24 hours. Values represent mean and SD of duplicate samples.

suggestive of a relationship between IKBKE activation and CYT387 treatment (Figure 2A and Figure 3D). Corroborating these findings, immortalized human mammary epithelial cells that expressed IKBKE (16) were more sensitive to CYT387 treatment than isogenic cells expressing a control vector, whereas ruxolitinib exposure had no effect on these cells (Figure 3E). Taken together, these observations reveal that CYT387, unlike ruxolitinib, selectively impairs TNBC cell viability in a manner that correlates with IKBKE expression.

Activity of CYT387 in TNBC directly involves inhibition of IKBKE signaling. To assess the direct consequences of CYT387 treatment on IKBKE activity, beyond CYT387's TBK1-specific effects (30), we transiently transfected 293T cells with IKBKE and measured downstream signaling pathways in the absence or presence of this inhibitor. Compared with expression of an EGFP control vector, exogenous overexpression of IKBKE primarily activated multiple STAT family members as well as p38α, and these effects were inhibited by CYT387 treatment (Supplemental Figure 5A). Both CYT387 and ruxolitinib inhibited IKBKE-induced Y705 pSTAT3 levels, consistent with suppression of autocrine cytokine signaling through JAK kinases (Figure 4A). IKBKE-induced pSTAT5 was also inhibited by CYT387 and ruxolitinib treatment (Supplemental Figure 5B). In contrast, when we measured phosphorylated p38α levels following treatment of IKBKE-expressing 293T cells or MDA-MB-468 cells with CYT387 or ruxolitinib, we were unable to observe significant changes in this marker, which suggests a lack of a direct relationship between p38α and IKBKE or JAK activity (Supplemental Figure 5, C and D).

We next examined the effects of CYT387 or ruxolitinib treatment on IKBKE-induced NF-κB signaling. IKBKE-induced p105 phosphorylation in 293T cells was inhibited by CYT387 treatment but not ruxolitinib treatment (Figure 4B). We confirmed that p105 was phosphorylated at a baseline low level in both MDA-MB-468 cells and MDA-MB231 cells and that CYT387 treatment also selectively inhibited phosphorylated p105 (p-p105) levels in these TNBC cell lines compared with ruxolitinib treatment (Figure 4C). IL-1β stimulation further induced S933 p105 phosphorylation in MDA-MB-468 cells, which was also selectively inhibited by CYT387 treatment, in contrast to ruxolitinib treatment, and resulted in p105 stabilization (Figure 4D). CYT387 treatment also suppressed IKBKE expression in MDA-MB-468 cells, in contrast to that of IKKβ or IKKα (Figure 4E). We further confirmed that CYT387 treatment inhibited p-p105, pSTAT3, and IKBKE levels in multiple other IKBKE-driven TNBC cell lines (Supplemental Figure 5, E and F). Thus, in contrast to ruxolitinib treatment, CYT387 treatment inhibits multiple components of the inflammatory signaling network that sustain proliferation and survival of this TNBC subtype.

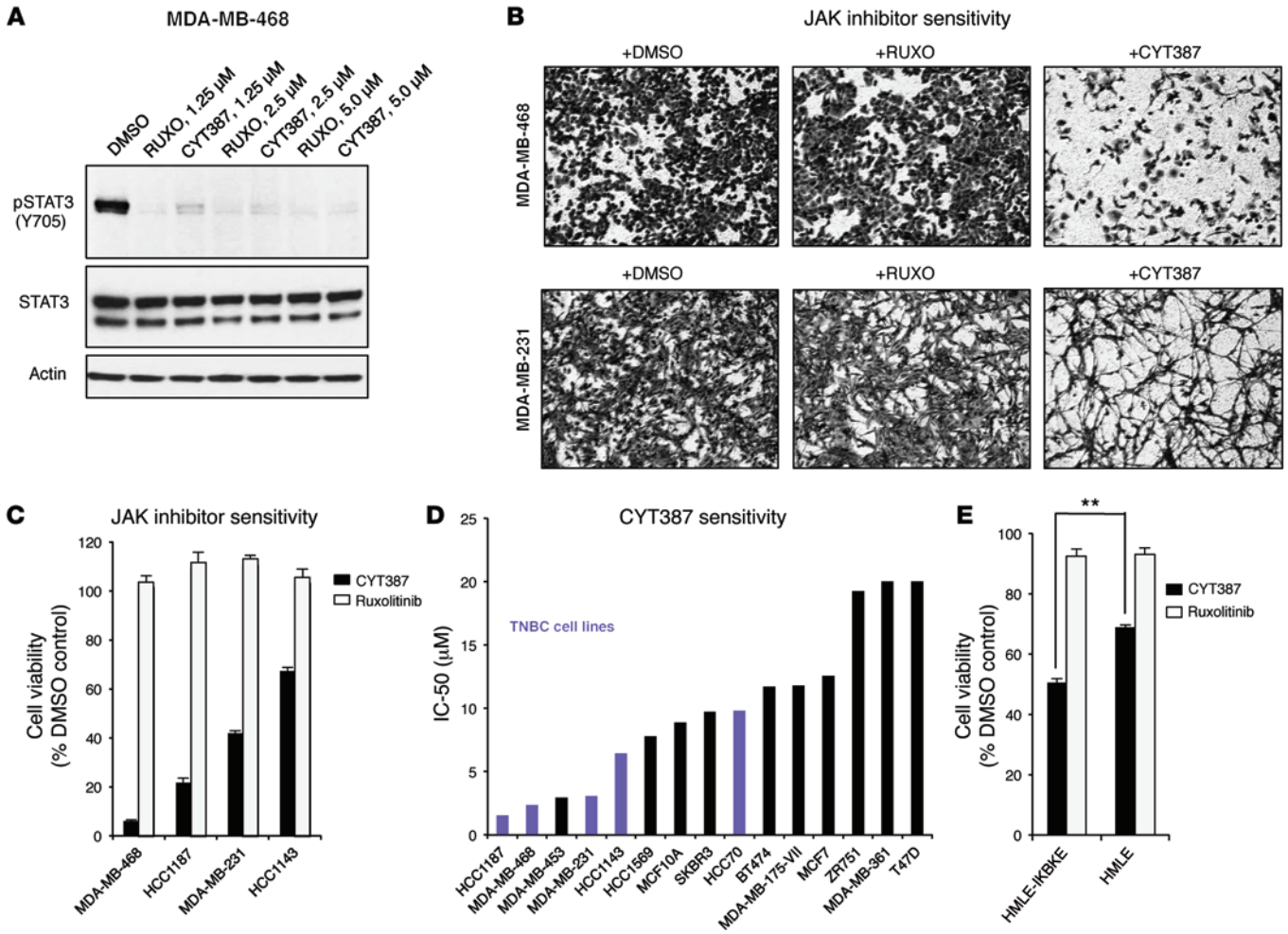

Figure 3. Sensitivity of IKBKE-expressing TNBC cells to CYT387. (**A**) Immunoblot of Y705 pSTAT3, total STAT3, and β-actin in MDA-MB-468 cells following ruxolitinib or CYT387 treatment at the indicated concentrations for 1 hour. (**B**) Phase-contrast microscopy (original magnification, ×10) of crystal violet–stained MDA-MB-468 or MDA-MB-231 cells treated with DMSO, 5 μM ruxolitinib, or 5 μM CYT387 for 3 days. (**C**) Relative viability by CTG assay of multiple IKBKE-driven TNBC cell lines following CYT387 or ruxolitinib treatment for 5 days, normalized to control DMSO treatment. Values represent mean and SEM of triplicate samples. (**D**) IC_{50} values for CYT387 treatment across a panel of 15 breast cancer cell lines treated with serial dilutions of CYT387 or DMSO as a control. Cell viability was measured after 5 days using CTG and normalized to values obtained from DMSO-treated cells. TNBC cell lines are indicated in purple. (**E**) Relative cell viability of immortalized human mammary epithelial cells (HMLE) isogenic for IKBKE expression (myristolated-Flag-IKBKE or vector control) treated with 5 μM CYT387 or ruxolitinib for 5 days, normalized to control DMSO treatment. Mean and SEM of triplicate samples shown. $^{**}P < 0.001$ by *t* test.

To examine more directly the role of IKBKE inhibition by CYT387 in TNBC proliferation and survival, we used a CYT387-resistant allele, IKBKE-Y88C, identified by homology to JAK2 (30, 35). We stably expressed the IKBKE-Y88C allele in MDA-MB-468 cells and selected the cells in the presence of 2.5 μM CYT387 for 3 weeks. We confirmed that the cells that emerged markedly overexpressed IKBKE-Y88C compared with control EGFP-expressing MDA-MB-468 cells (Figure 4F). CYT387 treatment of MDA-MB-468-IKBKE-Y88C cells failed to suppress IKBKE expression or baseline levels of p-p105, consistent with downstream resistance to this activity (Figure 4F). Treatment of MDA-MB468-IKBKE-Y88C cells with CYT387 resulted in enhanced proliferation and survival in vitro compared with control cells that expressed EGFP (Figure 4G). These observations confirm that inhibition of IKBKE by CYT387 directly contributes to its antiproliferative activity in IKBKE-driven TNBC cells.

CYT387 treatment disrupts IKBKE-induced protumorigenic cytokine expression. Given the unique ability of CYT387 to target this signaling network, we next tested its impact on autocrine cytokine expression. We collected media from 293T cells 24 hours following transient transfection with EGFP or IKBKE and analyzed levels of 36 different cytokines and chemokines using a cytokine antibody array. Enforced expression of IKBKE potently induced CCL5 levels in the media, consistent with what was observed at the mRNA level (Figure 2B), and was the dominant secreted factor at this time point (Figure 5A). IKBKE-dependent CCL5 production was completely abrogated by CYT387 treatment but was negligibly affected by ruxolitinib treatment (Figure 5A). To confirm these observations, we used ELISA to measure CCL5 levels in addition to those of IL-6 and found that IKBKE-induced CCL5 and IL-6 were strongly inhibited by CYT387 treatment, whereas they were only partially suppressed by ruxolitinib treat-

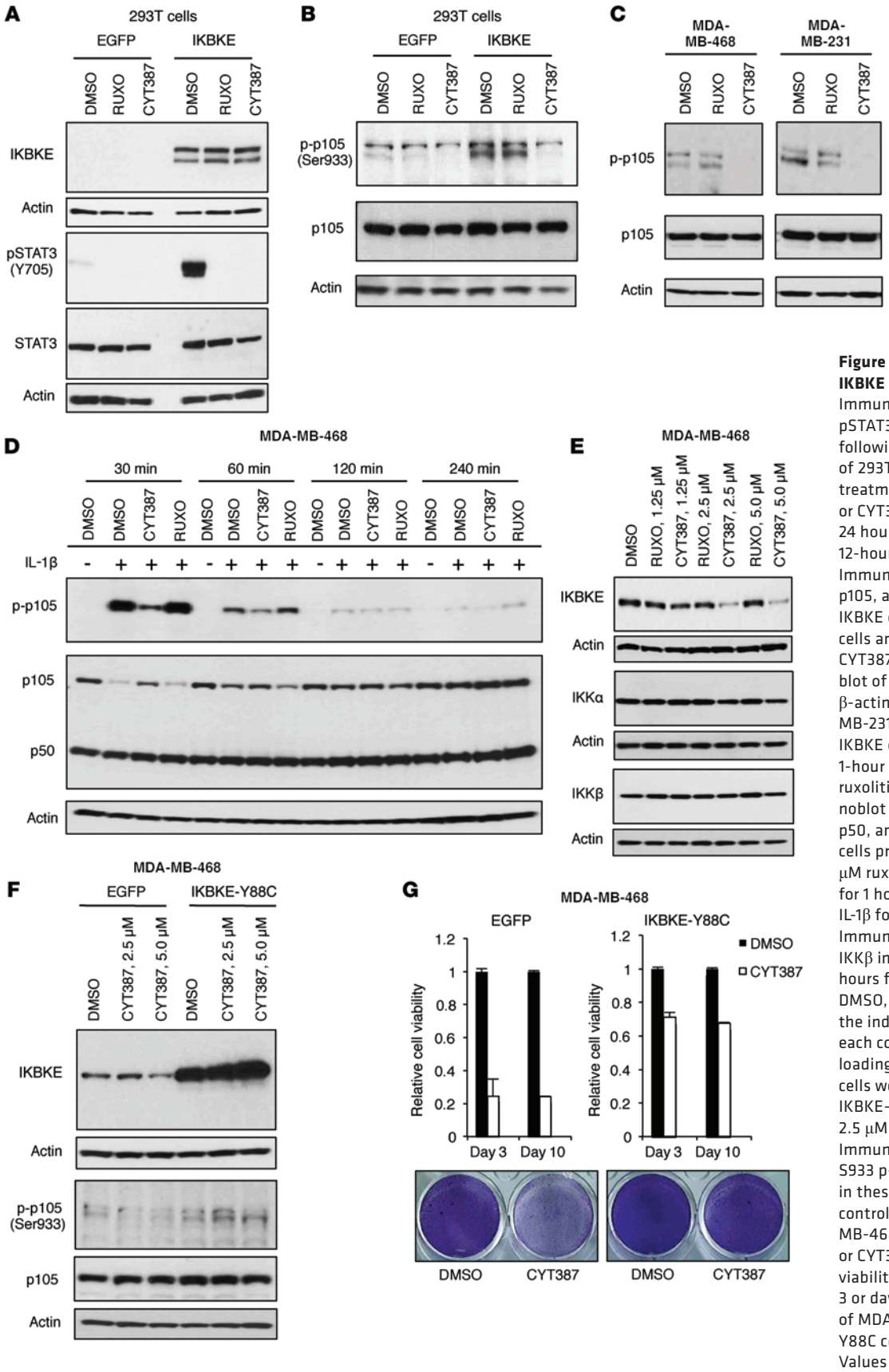

Figure 4. Inhibition of JAK and IKBKE signaling by CYT387. (**A**) Immunoblot of IKBKE, Y705 pSTAT3, total STAT3, and β-actin following transient transfection of 293T cells with IKBKE and treatment with 5 μM ruxolitinib or CYT387. Lysates were obtained 24 hours after transfection and 12-hour inhibitor treatment. (**B**) Immunoblot of S933 p-p105, p105, and β-actin following IKBKE overexpression in 293T cells and 5 μM ruxolitinib or CYT387 treatment. (**C**) Immunoblot of S933 p-p105, p105, and β-actin in MDA-MB-468 or MDA-MB-231 cells with endogenous IKBKE overexpression following 1-hour treatment with 5 μM ruxolitinib or CYT387. (**D**) Immunoblot of S933 p-p105, p105, p50, and β-actin in MDA-MB-468 cells pretreated with DMSO, 5 μM ruxolitinib, or 5 μM CYT387 for 1 hour and stimulated with IL-1β for the indicated times. (**E**) Immunoblot of IKBKE, IKKα, and IKKβ in MDA-MB-468 cells 24 hours following treatment with DMSO, ruxolitinib, or CYT387 at the indicated concentrations, each compared with β-actin as a loading control. (**F**) MDA-MB-468 cells were stably infected with IKBKE-Y88C and selected in 2.5 μM CYT387 for 3 weeks. Immunoblot shows IKBKE, S933 p-p105, p105, and β-actin in these cells compared with control EGFP-expressing MDA-MB-468 cells following DMSO or CYT387 treatment. (**G**) Cell viability measured by CTG on day 3 or day 10 following treatment of MDA-MB-468-EGFP or IKBKE-Y88C cells with DMSO or CYT387. Values were normalized to DMSO as a control and represent mean and SEM of triplicate samples. Crystal violet–stained wells are shown below.

ment (Figure 5B). These findings reveal that CYT387 treatment not only inhibits both STAT3- and IKBKE-induced p105 phosphorylation but also uniquely ablates the production of CCL5 and IL-6 following IKBKE overexpression.

We next assessed whether CYT387 inhibition of this network also impaired the production of CCL5 and IL-6 in TNBC cell lines. Treatment of MDA-MB468, MDA-MB231, HCC1187, or HCC70 cells with CYT387 in general prevented IL-1β–induced CCL5 and IL-6 (Figure 5C and Supplemental Figure 6A). To examine the consequences downstream of CCL5 and IL-6 production on TNBC proliferation, we first tested whether the addition of exogenous CCL5 and/or IL-6 rescued the viability of CYT387-treated MDA-MB-468 cells in 2D culture. We observed a modest but significant rescue following treatment with either cytokine or the combination of both ($P < 0.001$) (Supplemental Figure 6B). In contrast, in 3D culture, CCL5 and IL-6 not only promoted MDA-MB-468 cell migration and proliferation as effectively as EGF but they also completely rescued the inhibition of spheroid dispersal by CYT387 (Figure 5D). Taken together, these observations demonstrate that IKBKE-driven CCL5 and IL-6 directly contribute to TNBC migration and proliferation of tumor spheroids, which is disrupted by CYT387 treatment.

TBK1/IKBKE-regulated cytokines also influence the tumor microenvironment and angiogenesis in particular (36). We therefore used another 3D device optimized to study the effects of IKBKE-induced CCL5/IL-6 on HUVEC behavior in collagen (Figure 5E and ref. 37). First, we overexpressed IKBKE-WT in 293T cells, seeded them in the opposing channel, and found that expression of IKBKE-WT induced HUVEC migration, in contrast to EGFP and IKBKE-KD controls (Supplemental Figure 6C). Next, we directly supplemented media with CCL5 and IL-6 and observed that these cytokines induced both endothelial cell migration and proliferation (Figure 5F and Supplemental Figure 6D). Because of the proliferation, we tested whether cotreatment of CCL5/IL-6 with the MEK inhibitor GSK1120212 prevented this phenotype, and indeed HUVEC migration was abrogated (Figure 5F). Taken together, IKBKE-regulated CCL5 and IL-6 induce the proliferation and migration of TNBC and endothelial cells, consistent with both autocrine and paracrine tumor-promoting activities.

Inhibition of IKBKE by CYT387 contributes to its therapeutic potential in vivo. To determine efficacy of CYT387-based treatment in vivo, we first tested its therapeutic impact on MDA-MB-468 tumor xenograft growth and the relationship with IKBKE inhibition. After tumors were established in immunodeficient mice at an average volume of 50 mm^3, CYT387 was administered via daily oral gavage at a dose of 100 mg/kg (33). Compared with a vehicle control, CYT387 treatment at this dose effectively inhibited pSTAT3 expression in tumors (Figure 6A) and strongly suppressed tumor progression (Figure 6B). In consonance with our observations in vitro, CYT387 treatment did not affect the growth of MDA-MB-468 IKBKE-Y88C xenografts (Figure 6B).

We next explored single-agent CYT387 activity in a system that more closely recapitulates human tumor physiology using patient-derived breast cancer xenografts (PDXs). First, we examined therapy in two different Washington University human-in-mouse (WHIM) lines (WHIM4 and WHIM21) that were derived from patients with TNBC that overexpressed *IKBKE* (ref. 38 and Supplemental Figure 7A). Similar to what we observed following treatment of MDA-MB-468 xenografts, CYT387 treatment impaired the growth of established PDX WHIM4 tumors and WHIM21 tumors, the latter a particularly aggressive model that recurred rapidly following neoadjuvant doxorubicin/cyclophosphamide and paclitaxel chemotherapy (ref. 38 and Figure 6C). Inhibition of WHIM21 PDX growth was associated with disruption of human *IKBKE*, *CCL5*, and *IL6* expression, confirming effective interruption of autocrine cytokine signaling in these tumors (Figure 6D). Taken together, these findings reveal that inhibition of TBK1/IKBKE and JAK signaling by CYT387 suppresses protumorigenic cytokine expression and exhibits therapeutic potential for IKBKE-driven TNBC.

Synergistic response to combined CYT387 and GSK1120212 therapy. MEK inhibition in TNBC not only results in feedback activation of receptor tyrosine kinases but also induces cytokine expression, suggesting the possibility of synergy with CYT387 treatment (39). In addition the requirement of MEK signaling for CCL5/IL-6–induced proliferation/migration of endothelial cells (Figure 5F) indicated the potential for dual impairment of angiogenesis. We therefore treated established WHIM21 tumors with CYT387 (50 mg/kg/d), GSK1120212 (2.5 mg/kg/d), or combination CYT387/GSK1120212 therapy by oral gavage. The drug combination was well tolerated, and, in contrast to either of the single agents, markedly impaired tumor progression (Figure 7A). Indeed, several of the largest established tumors also showed evidence of tumor regression (Supplemental Figure 7B). We confirmed that dual CYT387 and GSK1120212 treatment effectively inhibited both phosphorylated ERK (pERK) and pSTAT3 levels in treated WHIM21 tumors, confirming suppression of multiple pathways by this drug combination in vivo (Figure 7B).

To assess the dose-dependent effect of this impressive activity, we further reduced CYT387 to 10 mg/kg daily and compared results with vehicle or high-dose ruxolitinib treatment (Supplemental Figure 6A). Treatment of WHIM21 tumors with just a 2-week course of low-dose CYT387/GSK1120212 led to marked and persistent inhibition of tumor progression at 4 weeks, in contrast to continuous vehicle or ruxolitinib treatment at 100 mg/kg daily over the entire time period (Supplemental Figure 8A). Response to this low-dose CYT387 regimen was also examined in WHIM12 PDX tumors, derived from a patient with TNBC with low *IKBKE* levels (Supplemental Figure 6A). WHIM12 tumors responded to CYT387/GSK1120212 treatment though not as dramatically as WHIM21 tumors, with some tumors progressing despite therapy (Supplemental Figure 8B).

In addition to their small size, we also noted that WHIM21 tumors treated with the combination of CYT387 and GSK-1120212 appeared particularly pale compared with vehicle- or single-agent–treated tumors (Figure 7C and Supplemental Figure 7C). We therefore performed a detailed histologic examination of treated tumors, including measures of angiogenesis. Whereas single-agent treatment with GSK1120212 showed preferential impairment of proliferation, as measured by Ki67 staining, and CYT387 modestly reduced microvascular density, the combination resulted in a striking inhibition of angiogene-

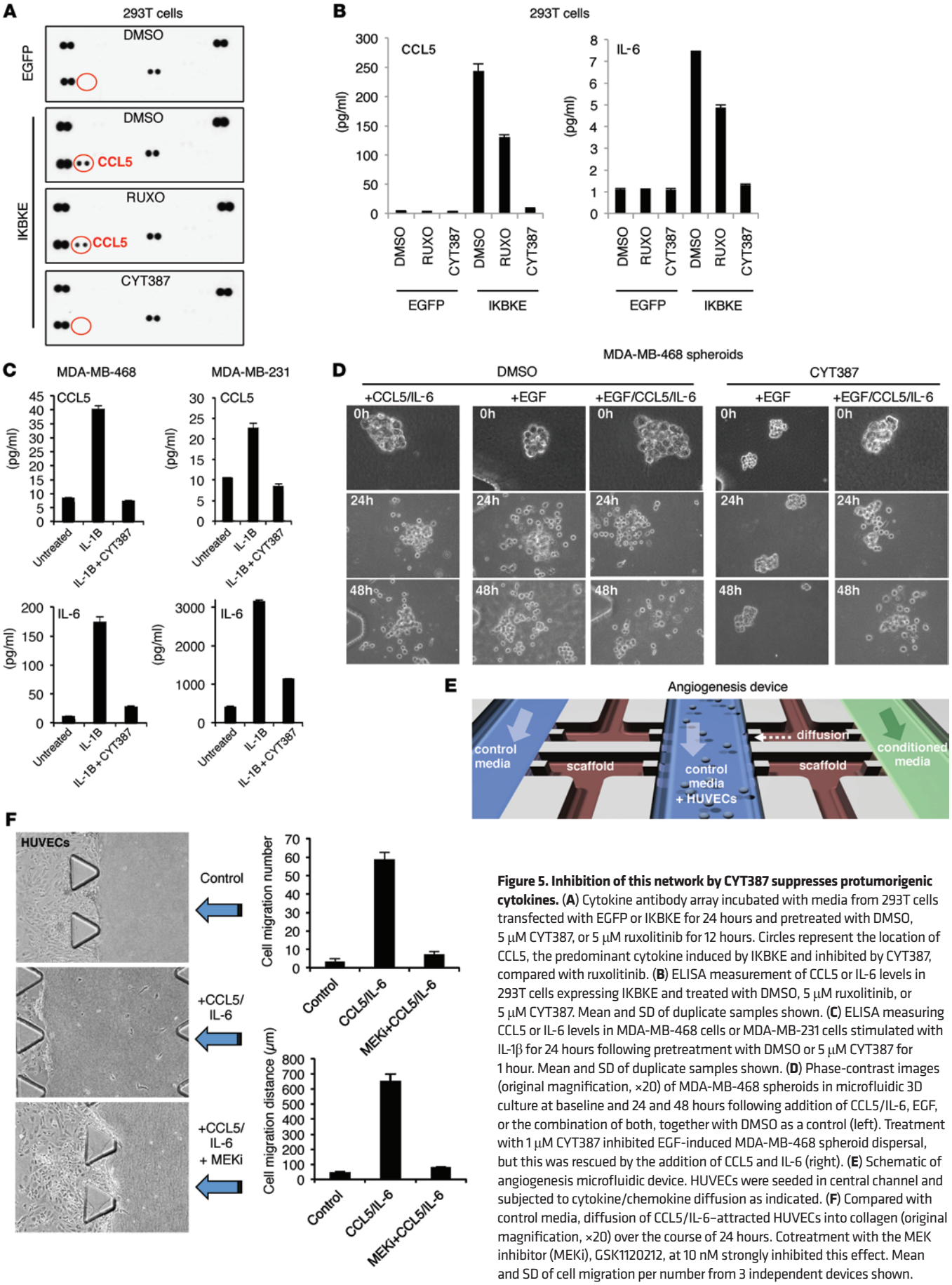

Figure 5. Inhibition of this network by CYT387 suppresses protumorigenic cytokines. (**A**) Cytokine antibody array incubated with media from 293T cells transfected with EGFP or IKBKE for 24 hours and pretreated with DMSO, 5 μM CYT387, or 5 μM ruxolitinib for 12 hours. Circles represent the location of CCL5, the predominant cytokine induced by IKBKE and inhibited by CYT387, compared with ruxolitinib. (**B**) ELISA measurement of CCL5 or IL-6 levels in 293T cells expressing IKBKE and treated with DMSO, 5 μM ruxolitinib, or 5 μM CYT387. Mean and SD of duplicate samples shown. (**C**) ELISA measuring CCL5 or IL-6 levels in MDA-MB-468 cells or MDA-MB-231 cells stimulated with IL-1β for 24 hours following pretreatment with DMSO or 5 μM CYT387 for 1 hour. Mean and SD of duplicate samples shown. (**D**) Phase-contrast images (original magnification, ×20) of MDA-MB-468 spheroids in microfluidic 3D culture at baseline and 24 and 48 hours following addition of CCL5/IL-6, EGF, or the combination of both, together with DMSO as a control (left). Treatment with 1 μM CYT387 inhibited EGF-induced MDA-MB-468 spheroid dispersal, but this was rescued by the addition of CCL5 and IL-6 (right). (**E**) Schematic of angiogenesis microfluidic device. HUVECs were seeded in central channel and subjected to cytokine/chemokine diffusion as indicated. (**F**) Compared with control media, diffusion of CCL5/IL-6–attracted HUVECs into collagen (original magnification, ×20) over the course of 24 hours. Cotreatment with the MEK inhibitor (MEKi), GSK1120212, at 10 nM strongly inhibited this effect. Mean and SD of cell migration per number from 3 independent devices shown.

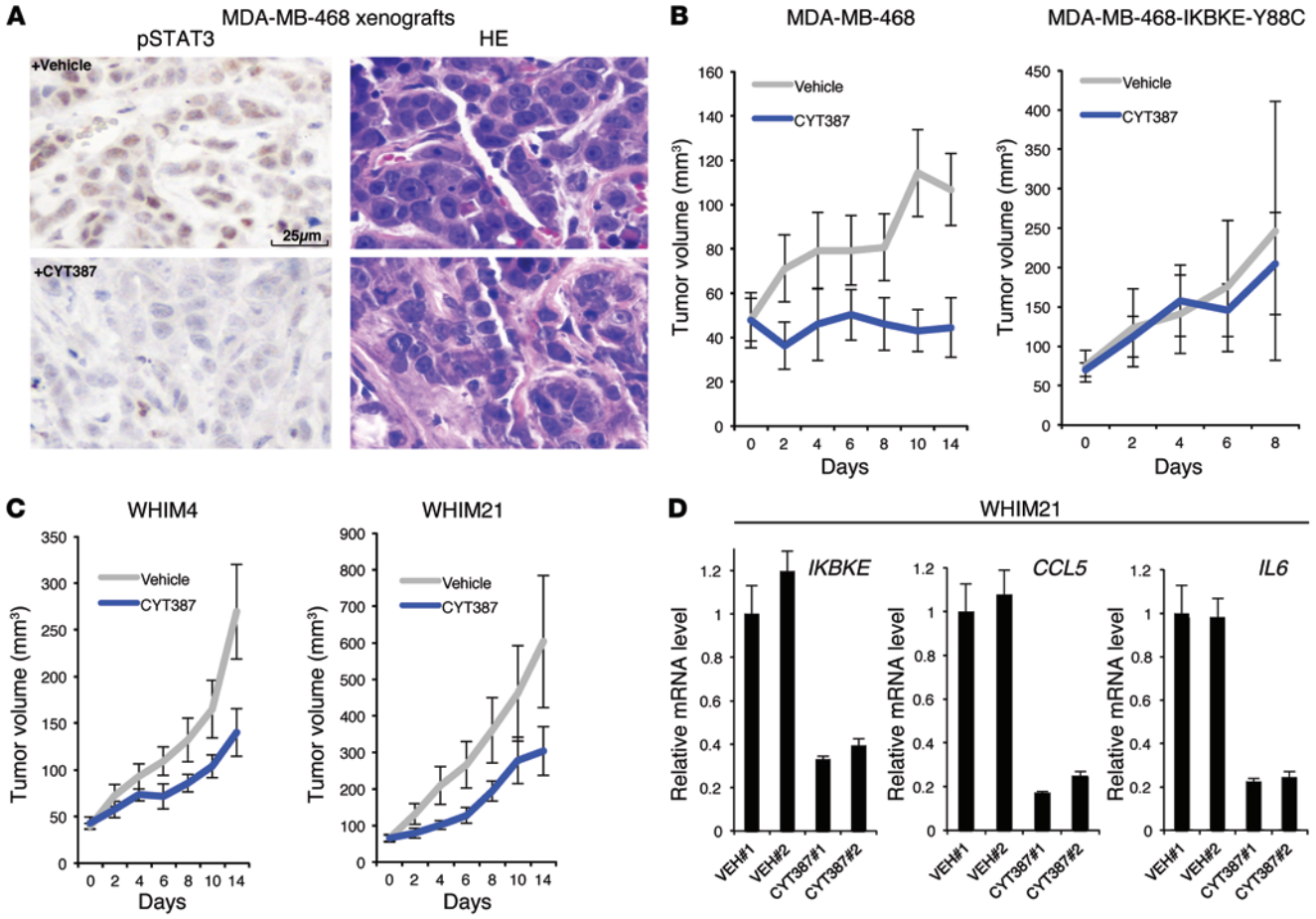

Figure 6. CYT387 inhibits IKBKE signaling and tumor progression in vivo. (**A**) MDA-MB-468 cells were implanted subcutaneously in nude mice, and following the development of established xenograft tumors, vehicle or CYT387 100 mg/kg was administered daily by oral gavage. Levels of pSTAT3 were measured by immunohistochemistry following short-term treatment. HE, hematoxylin eosin stain. Scale bar: 25 μM. (**B**) Mean tumor volume ± SEM following vehicle (n = 4) or CYT387 (n = 5) treatment over time in MDA-MB-468 or MDA-MB-468 IKBKE-Y88C xenografts. (**C**) Mean tumor volume ± SEM following vehicle (n = 5) or CYT387 100 mg/kg/d (n = 5) treatment over 14 days in WHIM4 and WHIM21 primary human tumor xenografts. (**D**) Relative mRNA levels of human *IKBKE*, *CCL5*, and *IL6* in WHIM21 tumors following short-term vehicle or CYT387 treatment. Values represent mean and SEM of triplicate samples from 2 different animals.

sis and profound tumor necrosis (Figure 7D and Supplemental Figure 9). Thus, antitumor activity of this drug combination was not only direct but was also related to the synergistic effects of cytokine and MEK inhibition on angiogenesis. Taken together, combined CYT387 and GSK1120212 treatment impairs tumor progression and angiogenesis and represents a promising novel therapy for this IKBKE-driven subtype of TNBC.

Discussion

TNBC has been defined by the lack of ER and HER2 expression, but several lines of evidence suggest that TNBCs are a heterogeneous set of breast cancers (40). Here, we identify a specific TNBC subset characterized by aberrant expression of the IKK-related kinase IKBKE and production of protumorigenic cytokines CCL5 and IL-6. These tumors show substantial overlap with the IM subtype of TNBC, recently identified by gene expression profiling studies (6). In contrast to luminal tumors, which exhibit *IKBKE* amplification (16), these triple-negative tumors exhibit inducible IKBKE expression associated with markers of IL-1 signaling and lymphocytic infiltration. Despite engagement of the JAK/STAT pathway (24), treatment with the potent and selective JAK1/2 inhibitor ruxolitinib was insufficient to impair viability of these TNBCs. Instead, another clinical stage JAK inhibitor, CYT387, impaired the proliferation of TNBC cells in vitro and prevented tumor spheroid dispersal in 3D culture. The efficacy of CYT387 was directly related to its additional ability to inhibit IKBKE activity and the production of protumorigenic cytokines, since exogenous CCL5 and/or IL-6, or expression of a CYT387 inhibitor–resistant allele of IKBKE, rescued these effects. These observations suggest a promising therapeutic option for a subset of patients with IKBKE-driven TNBC.

Integrative genomic studies identified a key role for aberrant IKBKE activation in breast cancer by virtue of its amplification in a subset of luminal tumors (16). IKBKE is unique among IKK family members in that cytokines such as IL-1 that promote NF-κB signaling (25) and STAT3 activation (41), which induces its expression. The finding that high level IKBKE expression in the IM subtype of TNBC was linked more closely to engagement of inflammatory

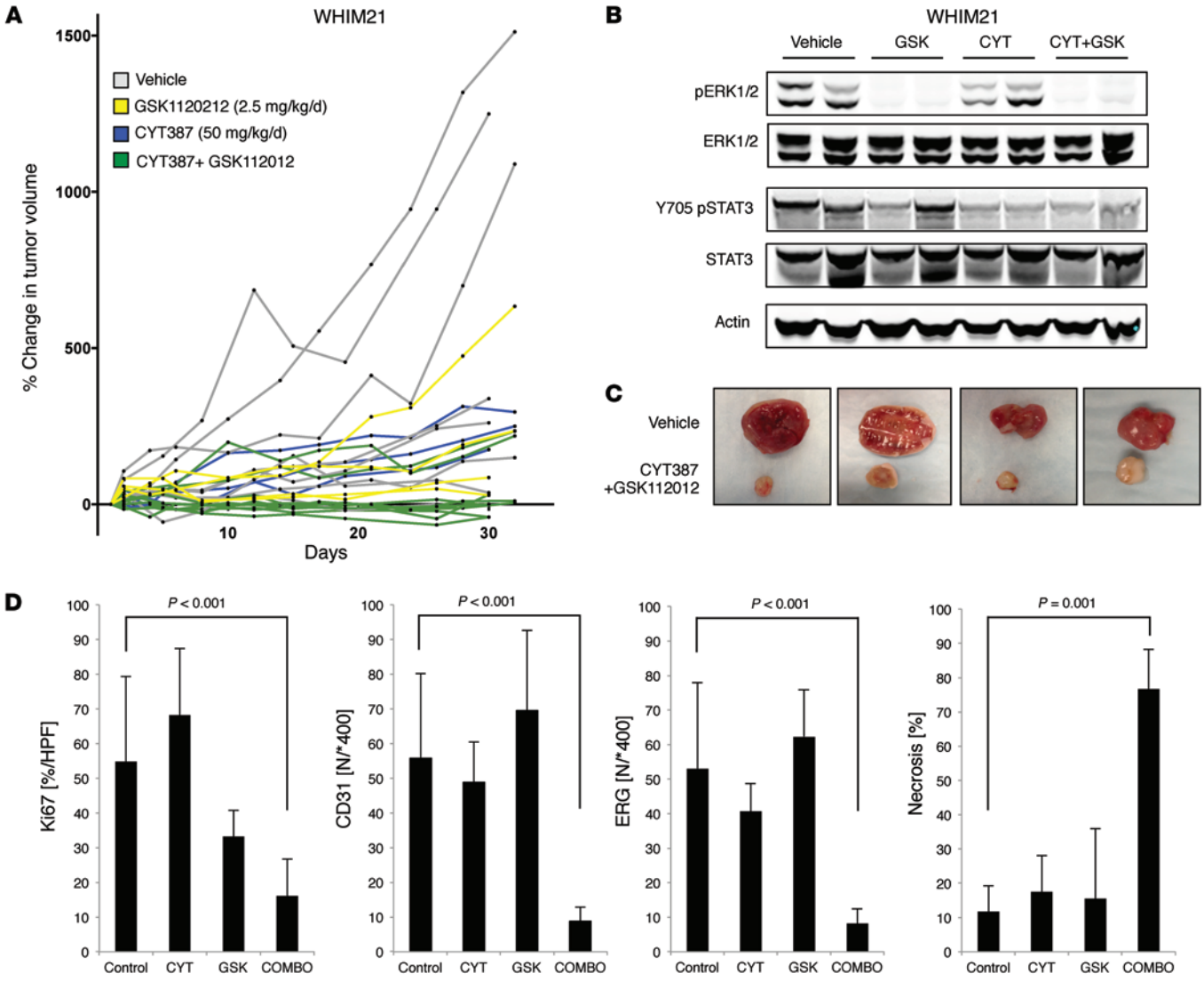

Figure 7. Activity of CYT387/GSK1120212 combination therapy in an aggressive TNBC PDX model. (**A**) Spider plot depicting the percentage of change in tumor volume of individual WHIM21 tumors treated with vehicle (n = 8), 50 mg/kg/d CYT387 (n = 3), 2.5 mg/kg/d GSK1120212 (n = 4), or CYT387 and GSK1120212 (n = 9). (**B**) Immunoblot of pERK1/2, ERK1/2, Y705 pSTAT3, STAT3, and β-actin levels in tumors from vehicle-treated mice or 2 different mice treated short term with vehicle, CYT387 (CYT), GSK1120212 (GSK), or the combination of CYT387 and GSK1120212 (CYT+GSK). (**C**) Representative WHIM21 tumors dissected from vehicle or CYT387/GSK1120212-treated mice after 30 days. (**D**) Quantification of proliferation (Ki67), microvascular density (CD31 or ERG), and tumor necrosis of tumors dissected after 30 days of the indicated treatments. Data represent mean and SD values quantified from ≥5 distinct tumor regions from vehicle- (n = 3), CYT387- (n = 2), GSK1120212- (n = 2), or CYT387/GSK1120212-treated (n = 2) mice. COMBO, CYT387 and GSK1120212.

signaling than to genomic amplification reveals an alternative route to oncogenic IKBKE activation in TNBC, similar to what was recently described in a subset of lung cancers (41). While IKBKE drives the expression of these cytokines, engagement of other kinases, including TBK1, likely also contributes to inflammatory signaling in this subtype, since multitargeted IKBKE, TBK1, and JAK signaling was required to disrupt this circuit. Since other non-TNBC breast cancers also overexpress IKBKE and also activate TBK1 signaling (42), such tumors could also respond to TBK1/IKBKE and JAK inhibition by CYT387.

Our studies also identified key downstream roles for CCL5 and IL-6 as IKBKE-driven mediators of cell proliferation, survival, and migration of breast cancer cells. CCL5 induces pleiotropic effects on NF-κB target gene expression (43) and AKT activation (44, 45) and, like IL-6, directly engages JAK/STAT signaling (46). Thus, NF-κB and STAT3 not only induce the production of CCL5 and IL-6, but they also engage these same pathways and activate IKBKE expression itself (41) to amplify and sustain their expression as components of an inflammatory circuit (30). Induction of CCL5, which promotes cell survival and metastasis, has also been observed in breast cancer following coculture with mesenchymal stem cells (44). These findings suggest that paracrine effects due to interactions within tumor microenvironment likely facilitate engagement of this signaling pathway. Since we observed an important role of IL-1 signaling in driving this phenotype, it will be interesting to examine whether

the source of this cytokine in primary breast tumors is derived from mesenchymal stem cells, tumor-associated macrophages, and/or other cell types in the tumor microenvironment.

IKBKE-induced CCL5 and IL-6 expression also stimulated HUVEC proliferation, consistent with a previous report showing that conditioned media from TBK1-transfected cells promotes vascular cell proliferation (36). Our findings confirm and extend these data, revealing a particular role for MEK signaling downstream of these cytokines in mediating endothelial cell proliferation and identifying synergistic inhibition of angiogenesis by CYT387 and MEK inhibition in vivo. Cytokines such as CCL5 may also promote TNBC growth by influencing the local immune microenvironment, since it also influences recruitment of myeloid-derived suppressor cells to tumors and promotes local immunosuppression (47). Analysis of such cells is challenging in PDX models, given the altered immune background of nude mice, but will be important to evaluate in future studies. Thus, CYT387 therapy may be particularly effective in vivo due to the additional disruption of these tumor-stromal interactions.

Clinical trials of selective JAK1/2 inhibitors such as ruxolitinib have been initiated in patients with breast cancer (48). While JAK/STAT signaling is clearly active in this subset of TNBC, our data suggest that JAK inhibition alone may not be sufficient to disrupt this cytokine circuit. Furthermore, although certain markers, such as $CD44^+CD24^-$ positivity or the IM gene expression profile, have been associated with this particular TNBC phenotype (6, 24, 49), the underlying driver of cytokine activation in these cancers has remained elusive. The identification of IKBKE as a key driver of this cytokine signaling network provides not only provides an additional marker of this emerging TNBC subtype but also a discrete molecular target. It is also becoming increasingly apparent that targeting the source of these upstream cytokines represents an equally important strategy to target TNBC growth compared with JAK inhibition (50). Indeed, our data suggest that the capacity of CYT387 to inhibit TBK1/IKBKE and JAK/STAT signaling, resulting in a particularly potent anti-cytokine effect, may be advantageous over more selective JAK1/2 inhibitors.

It is also clear that inhibition of any one pathway in genetically complex tumors typically results in feedback signaling that limits the effectiveness of single-agent therapy. Indeed, treatment of TNBC with MEK inhibitors leads to feedback activation of both receptor tyrosine kinase signaling and cytokines (39). Conversely, CYT387 treatment modestly inhibited IKBKE-driven TNBC growth as a single agent but dramatically impaired tumor growth and angiogenesis when combined with a MEK inhibitor, revealing cooperativity of targeting these pathways in vivo. Combination CYT387 and MEK inhibitor therapy was also synergistic and resulted in tumor regressions in aggressive *Kras-p53* mutated murine lung cancer (30). Since cytokine signaling similarly limits the efficacy of PI3K/mTOR inhibitors in breast cancer (51), further strategies for combination therapy may be possible. Regardless, the particularly impressive synergy of CYT387 and GSK1120212 in an aggressive PDX model, coupled with their advanced stages of clinical development, provides a strong rationale for pursuing clinical trials of this drug combination in patients with TNBC.

Methods

Gene expression profiling. Analyses were performed using TCGA data (2) and applied single-sample gene set enrichment analysis of an IL-1 signature as described previously (26, 52). For details, see the Supplemental Methods.

Cell culture. Breast cancer cell lines and 293T cells were cultured using standard conditions. MDA-MB-468 cells were maintained in the absence of CO_2. MDA-MB-468 tumor spheroids were generated and assayed in 3D culture as described previously (34). Detailed methods are described in the Supplemental Methods.

Immunoblotting and ELISA. Immunoblotting was performed according to standard protocols. Proteome Profiler and Cytokine Antibody Arrays were from R&D Systems. The Proteome Profiler Human Cytokine Array Kit, Panel A (catalog no. ARY005), the Human CCL5/Rantes Quantikine ELISA Kit (catalog no. DRN00B), and the Human IL-6 ELISA Kit (catalog no. D6050) were also purchased from R&D Systems. Details are provided in the Supplemental Methods.

ORF and shRNA expression. 293T cells were transiently transfected with the indicated ORF expression constructs using FuGENE 6 (Promega). Using stable lentiviral transduction as previously described (52), shRNA (shIKBKE-1, shIKBKE-2, shGFP) was successfully expressed and its effects on the various breast cancer cell lines were analyzed using stable lentiviral transduction as described previously (52). For detailed methods and shRNA sequences see the Supplemental Methods.

Quantitative real-time PCR. mRNA was purified and qRT-PCR was performed according to a standard protocol using the LightCycler 480 SYBR Green I Master (Roche). Data were normalized to 36B4. For detailed methods and primer sequences see the Supplemental Methods.

Animal studies. Patient-derived human breast xenografts were cultured as described previously (38, 53). pSTAT3 immunohistochemistry and pSTAT3/pERK immunoblotting were performed following short-term treatment with CYT387. Tumor measurement was conducted in a blinded fashion over time. Details are provided in the Supplemental Methods.

Statistics. Statistical analysis was carried out using an IBM software package, SPSS V.22.0. Cell viability data are presented as mean ± SEM. Histology data are presented as mean ± SD of independent results. Overall differences among the 4 groups (vehicle, GSK1120212, CYT387, and CYT387 plus GSK112012) for all variables were determined by ANOVA. Differences between groups were examined using the nonparametric independent-samples *t* test to determine the statistical significance. Two-sided *P* values of less than 0.05 were considered statistically significant.

Study approval. Human breast cancer tissues for the present studies were obtained via core needle, skin punch biopsy, or surgical resection following informed consent and processed in compliance with NIH regulations and with approval from the Institutional Review Board at Washington University in St. Louis. All mouse experiments were conducted in accord with a Washington University Institutional Animal Care and Use Committee–approved protocol.

Acknowledgments

We thank the HAMLET core for assistance with WHIM tumor propagation and the shRNA facility (RNAi Consortium, Children's Discovery Institute, and the Genome Institute) at Washington University School of Medicine. We thank Mahjobeh Rahimian Mashhadi and Yaser Masoudnia for assistance with 3D culture imaging.

This work was supported in part by NIH grant T32 CA009621 and the US Department of Defense Breast Cancer Award W81XWH-13-1-0029 (to T.U. Barbie), NIH grants P01 CA154303 and R01 CA130988 (to W.C. Hahn), and NIH grant K08 CA138918-01A1 (to D.A. Barbie). D.A. Barbie is supported by V Scholar, Gloria Spivak Faculty, GTM Fund for Lung Cancer Research, and Friends of the Dana-Farber Cancer Institute Awards.

Address correspondence to: William E. Gillanders, 660 S. Euclid Avenue, Box 8109, St. Louis, Missouri 63110, USA. Phone: 314.362.2280; E-mail: gillandersw@wudosis.wustl.edu. Or to: David A. Barbie, 450 Brookline Avenue, D819, Boston, Massachusetts 02215, USA. Phone: 617.632.2641; E-mail: dbarbie@partners.org. Or to: William C. Hahn, 450 Brookline Avenue, D1538, Boston, Massachusetts 02215, USA. Phone: 617.632.6049; E-mail: William_Hahn@dfci.harvard.edu.

1. Hudis CA, Gianni L. Triple-negative breast cancer: an unmet medical need. *Oncologist*. 2011;16(suppl 1):1–11.
2. Koboldt DC, et al. Comprehensive molecular portraits of human breast tumours. *Nature*. 2012;490(7418):61–70.
3. Foulkes WD, Smith IE, Reis-Filho JS. Triple-negative breast cancer. *N Engl J Med*. 2010;363(20):1938–1948.
4. Creighton CJ, et al. Residual breast cancers after conventional therapy display mesenchymal as well as tumor-initiating features. *Proc Natl Acad Sci U S A*. 2009;106(33):13820–13825.
5. Hennessy BT, et al. Characterization of a naturally occurring breast cancer subset enriched in epithelial-to-mesenchymal transition and stem cell characteristics. *Cancer Res*. 2009;69(10):4116–4124.
6. Lehmann BD, et al. Identification of human triple-negative breast cancer subtypes and preclinical models for selection of targeted therapies. *J Clin Invest*. 2011;121(7):2750–2767.
7. Shen RR, Hahn WC. Emerging roles for the non-canonical IKKs in cancer. *Oncogene*. 2011;30(6):631–641.
8. Fitzgerald KA, et al. IKKepsilon and TBK1 are essential components of the IRF3 signaling pathway. *Nat Immunol*. 2003;4(5):491–496.
9. Hemmi H, et al. The roles of two IkappaB kinase-related kinases in lipopolysaccharide and double stranded RNA signaling and viral infection. *J Exp Med*. 2004;199(12):1641–1650.
10. McWhirter SM, Fitzgerald KA, Rosains J, Rowe DC, Golenbock DT, Maniatis T. IFN-regulatory factor 3-dependent gene expression is defective in Tbk1-deficient mouse embryonic fibroblasts. *Proc Natl Acad Sci U S A*. 2004;101(1):233–238.
11. Sharma S, tenOever BR, Grandvaux N, Zhou GP, Lin R, Hiscott J. Triggering the interferon antiviral response through an IKK-related pathway. *Science*. 2003;300(5622):1148–1151.
12. Tenoever BR, Ng SL, Chua MA, McWhirter SM, Garcia-Sastre A, Maniatis T. Multiple functions of the IKK-related kinase IKKepsilon in interferon-mediated antiviral immunity. *Science*. 2007;315(5816):1274–1278.
13. Ng SL, et al. IkappaB kinase epsilon (IKK(epsilon)) regulates the balance between type I and type II interferon responses. *Proc Natl Acad Sci U S A*. 2011;108(52):21170–21175.
14. Sankar S, Chan H, Romanow WJ, Li J, Bates RJ. IKK-i signals through IRF3 and NFkappaB to mediate the production of inflammatory cytokines. *Cell Signal*. 2006;18(7):982–993.
15. Adli M, Baldwin AS. IKK-i/IKKε controls constitutive, cancer cell-associated NF-κB activity via regulation of Ser-536 p65/RelA phosphorylation. *J Biol Chem*. 2006;281(37):26976–26984.
16. Boehm JS, et al. Integrative genomic approaches identify IKBKE as a breast cancer oncogene. *Cell*. 2007;129(6):1065–1079.
17. Eddy SF, et al. Inducible IκB kinase/IκB kinase ε expression is induced by CK2 and promotes aberrant nuclear factor-κB activation in breast cancer cells. *Cancer Res*. 2005;65(24):11375–11383.
18. Hutti JE, et al. Phosphorylation of the tumor suppressor CYLD by the breast cancer oncogene IKKε promotes cell transformation. *Mol Cell*. 2009;34(4):461–472.
19. Shen RR, Zhou AY, Kim E, Lim E, Habelhah H, Hahn WC. IκB kinase epsilon phosphorylates TRAF2 to promote mammary epithelial cell transformation. *Mol Cell Biol*. 2012;32(23):4756–4768.
20. Li L, Shaw PE. Autocrine-mediated activation of STAT3 correlates with cell proliferation in breast carcinoma lines. *J Biol Chem*. 2002;277(20):17397–17405.
21. Berishaj M, et al. Stat3 is tyrosine-phosphorylated through the interleukin-6/glycoprotein 130/Janus kinase pathway in breast cancer. *Breast Cancer Res*. 2007;9(3):R32.
22. Walker SR, et al. Reciprocal effects of STAT5 and STAT3 in breast cancer. *Mol Cancer Res*. 2009;7(6):966–976.
23. Hedvat M, et al. The JAK2 inhibitor AZD1480 potently blocks Stat3 signaling and oncogenesis in solid tumors. *Cancer Cell*. 2009;16(6):487–497.
24. Marotta LL, et al. The JAK2/STAT3 signaling pathway is required for growth of CD44CD24 stem cell-like breast cancer cells in human tumors. *J Clin Invest*. 2011;121(7):2723–2735.
25. Shimada T, et al. IKK-i, a novel lipopolysaccharide-inducible kinase that is related to IκB kinases. *Int Immunol*. 1999;11(8):1357–1362.
26. Jura J, et al. Identification of interleukin-1 and interleukin-6-responsive genes in human monocyte-derived macrophages using microarrays. *Biochim Biophys Acta*. 2008;1779(6):383–389.
27. Smiljanovic B, et al. The multifaceted balance of TNF-α and type I/II interferon responses in SLE and RA: how monocytes manage the impact of cytokines. *J Mol Med (Berl)*. 2012;90(11):1295–1309.
28. Iglesia MD, et al. Prognostic B-cell signatures using mRNA-seq in patients with subtype-specific breast and ovarian cancer. *Clin Cancer Res*. 2014;20(14):3818–3829.
29. Barretina J, et al. The Cancer Cell Line Encyclopedia enables predictive modelling of anticancer drug sensitivity. *Nature*. 2012;483(7391):603–607.
30. Zhu Z, et al. Inhibition of KRAS-driven tumorigenicity by interruption of an autocrine cytokine circuit. *Cancer Discov*. 2014;4(4):452–465.
31. Verstovsek S, et al. A double-blind, placebo-controlled trial of ruxolitinib for myelofibrosis. *N Engl J Med*. 2012;366(9):799–807.
32. Pardanani A, et al. Safety and efficacy of CYT387, a JAK1 and JAK2 inhibitor, in myelofibrosis. *Leukemia*. 2013;27(6):1322–1327.
33. Tyner JW, et al. CYT387, a novel JAK2 inhibitor, induces hematologic responses and normalizes inflammatory cytokines in murine myeloproliferative neoplasms. *Blood*. 2010;115(25):5232–5240.
34. Aref AR, et al. Screening therapeutic EMT blocking agents in a three-dimensional microenvironment. *Integr Biol (Camb)*. 2013;5(2):381–389.
35. Weigert O, et al. Genetic resistance to JAK2 enzymatic inhibitors is overcome by HSP90 inhibition. *J Exp Med*. 2012;209(2):259–273.
36. Czabanka M, Korherr C, Brinkmann U, Vajkoczy P. Influence of TBK-1 on tumor angiogenesis and microvascular inflammation. *Front Biosci*. 2008;13:7243–7249.
37. Shin Y, et al. Microfluidic assay for simultaneous culture of multiple cell types on surfaces or within hydrogels. *Nat Protoc*. 2012;7(7):1247–1259.
38. Li S, et al. Endocrine-therapy-resistant ESR1 variants revealed by genomic characterization of breast-cancer-derived xenografts. *Cell Rep*. 2013;4(6):1116–1130.
39. Duncan JS, et al. Dynamic reprogramming of the kinome in response to targeted MEK inhibition in triple-negative breast cancer. *Cell*. 2012;149(2):307–321.
40. Lehmann BD, Pietenpol JA. Identification and use of biomarkers in treatment strategies for triple negative breast cancer subtypes. *J Pathol*. 2014;232(2):142–150.
41. Guo J, et al. IKBKE is induced by STAT3 and tobacco carcinogen and determines chemosensitivity in non-small cell lung cancer. *Oncogene*. 2013;32(2):151–159.
42. Deng T, et al. shRNA kinome screen identifies TBK1 as a therapeutic target for HER2+ breast cancer. *Cancer Res*. 2014;74(7):2119–2130.
43. Fischer FR, Luo Y, Luo M, Santambrogio L, Dorf ME. RANTES-induced chemokine cascade in dendritic cells. *J Immunol*. 2001;167(3):1637–1643.
44. Karnoub AE, et al. Mesenchymal stem cells within tumour stroma promote breast cancer metastasis. *Nature*. 2007;449(7162):557–563.
45. Tyner JW, et al. CCL5-CCR5 interaction provides antiapoptotic signals for macrophage survival during viral infection. *Nat Med*. 2005;11(11):1180–1187.
46. Wong M, et al. Rantes activates Jak2 and Jak3 to regulate engagement of multiple signaling pathways in T cells. *J Biol Chem*. 2001;276(14):11427–11431.
47. Zhang Y, et al. A novel role of hematopoietic CCL5 in promoting triple-negative mammary tumor progression by regulating generation of myeloid-derived suppressor cells. *Cell Res*. 2013;23(3):394–408.
48. Quintas-Cardama A, Verstovsek S. Molecular pathways: Jak/STAT pathway: mutations, inhibitors, and resistance. *Clin Cancer Res*.

2013;19(8):1933–1940.
49. Tiezzi DG, et al. CD44+/CD24- cells and lymph node metastasis in stage I and II invasive ductal carcinoma of the breast. *Med Oncol*. 2012;29(3):1479–1485.
50. Hartman ZC, et al. Growth of triple-negative breast cancer cells relies upon coordinate autocrine expression of the proinflammatory cytokines IL-6 and IL-8. *Cancer Res*. 2013;73(11):3470–3480.
51. Britschgi A, et al. JAK2/STAT5 inhibition circumvents resistance to PI3K/mTOR blockade: a rationale for cotargeting these pathways in metastatic breast cancer. *Cancer Cell*. 2012;22(6):796–811.
52. Barbie DA, et al. Systematic RNA interference reveals that oncogenic KRAS-driven cancers require TBK1. *Nature*. 2009;462(7269):108–112.
53. Ma CX, et al. Targeting Chk1 in p53-deficient triple-negative breast cancer is therapeutically beneficial in human-in-mouse tumor models. *J Clin Invest*. 2012;122(4):1541–1552.